

High-Energy Neutron Radiography as a Tool for Stockpile Surveillance	134
--	-----

Proton Radiography Experiments at LANSCE	138
--	-----



High-Energy Neutron Radiography as a Tool for Stockpile Surveillance

T.N. Taddeucci (LANSCE Division), A.B. Kaye (X Division), T.N. Claytor, C.L. Faust, T.O. Davis (ESA Division), T.E. McDonald (P Division)

High-energy neutron radiography has the potential to detect details in light materials contained within massive objects. However, practical applications in neutron radiography will require a suitably intense neutron source and an efficient detector system. We have been using the Target-4 spallation neutron source at the LANSCE WNR facility to test neutron imaging and computed tomography (CT) techniques. Our measurements show that high-energy neutron radiography yields a level of contrast and resolution adequate to address specific stockpile surveillance needs.

The Challenge of High-Energy Neutron Radiography

A variety of radiographic techniques are available for applications in stockpile surveillance. The type of radiation best suited for a particular application (e.g., x-rays, gamma-rays, protons, and neutrons) depends on the resolution, count-rate, mass-sensitivity, and portability requirements of the problem at hand.

Matter is most transparent to neutrons having energies above several MeV. The neutron total cross section for all elements goes through a minimum for neutron energies near 300 MeV. Neutrons in this energy region can easily penetrate thick objects. Because neutrons interact via the strong interaction—that is, they scatter from the neutrons and protons in the atomic nucleus rather than the surrounding electron shells—sensitivity to light elements such as hydrogen is retained. This is in contrast to x-rays and gamma rays, which scatter primarily from electrons. High-energy neutrons may therefore be used in applications that require the inspection of hydrogenous layers shielded by heavier materials.

Reconstructing Radiographic Images in Three Dimensions

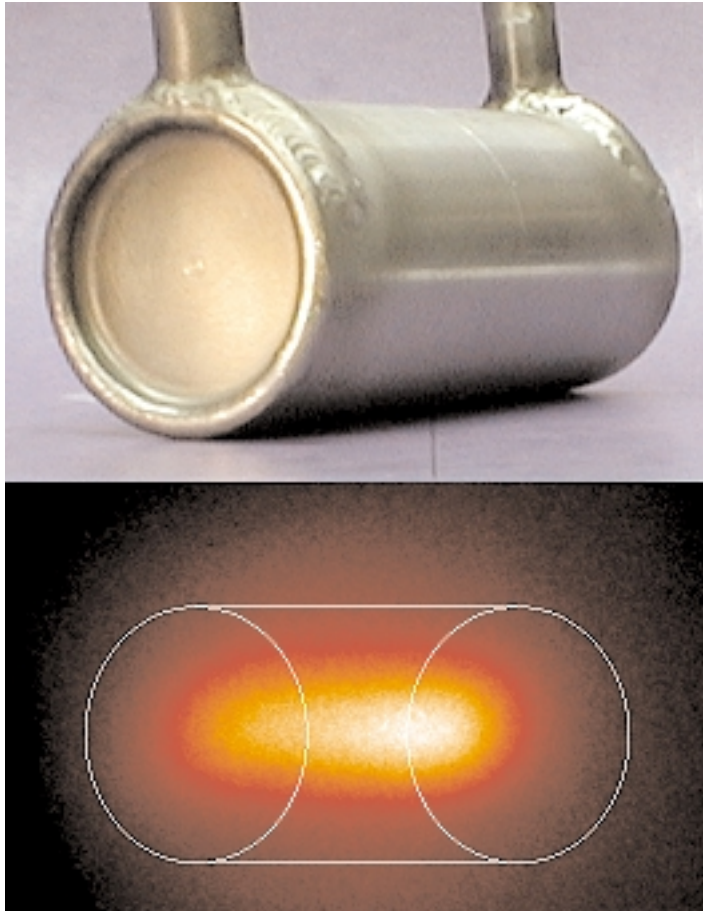
CT imaging reconstructs a three-dimensional image of an object (or equivalently, a set of two-dimensional cross-sectional slices) from a set of two-dimensional radiographic images. Several obstacles, however, must be overcome for CT imaging to become practical using high-energy neutrons. First, efficient neutron imaging detectors with good spatial resolution must be developed. The low cross section that makes matter relatively

transparent to high-energy neutrons also makes high-energy neutrons hard to detect. Second, an intense source of high-energy neutrons is required. Sufficiently high detector efficiency and source intensity are required to obtain detailed CT images in a reasonable amount of time. Finally, an acceptable level of mass sensitivity (image contrast) and resolution must be demonstrated. The contrast and resolution in an image are affected by the physics of the scattering process in the object being studied and by the neutron detector, finite size and geometry of the neutron source, and background radiation (i.e., gamma rays and x-rays produced by the neutron source).

Initially, we demonstrated and measured the contrast and resolution of CT images using the WNR Target-4 spallation neutron source at LANSCE. This source produces a broad spectrum of neutrons ranging in energy from sub-MeV to several-hundred MeV and is therefore well suited for testing a variety of neutron-imaging techniques. With this neutron source, we accomplished the following:

- tested two imaging systems—storage-phosphor image plates and amorphous silicon panels;
- detected holes in 20-mil Mylar sheets (75 mg/cm²) and 31-mil plastic drafting templates (96 mg/cm²) sandwiched between 3/4-in. iron plates; layers of aluminum, lead, and iron; and a 2-in.-thick uranium cube;
- performed neutron-activation measurements on a depleted-uranium (D₃₈) alloy cube and compared them to Monte Carlo estimates of activation products;
- used the intensity profile from the neutron shadow of the D₃₈ cube to obtain a measurement of the combined source plus image-plate resolution;
- used a brass "pinhole" collimator to produce a neutron pinhole image of the WNR Target-4 source, which allowed us to unfold the target contribution to the overall resolution and obtain the resolution of the detector (image plates) alone; and
- demonstrated CT imaging of a flat-plate object using storage phosphor image plates.

The pinhole image of WNR Target-4 (Fig. 1) provides a dramatic example of the difference between unmoderated high-energy neutron sources and moderated thermal cold-neutron sources that produce diffuse beams.



↑ **Fig. 1.** Replica of WNR Target-4 (top image). Target-4 is a 3-cm-diam, 7.5-cm-long tungsten cylinder surrounded by a water-cooling jacket. Neutron-pinhole image of Target-4 (bottom image). An outline of the inner tungsten cylinder is superimposed on the neutron image. In this image, the 800-MeV proton beam enters from the right.

The unmoderated Target-4 source yields neutrons that (for the most part) emerge in straight lines from their point of production. In this case, the laws of geometric optics apply and pinhole images can be formed in a manner directly analogous to light rays. For our measurement, we used a 27-cm-long brass collimator (Fig. 2) with a central aperture tapering to 1.6 mm at the center. This brass pinhole was located on the WNR 4FP30L flight path at a distance of 19 m from the target. The image was captured on storage-phosphor image plates located 40 m from the target.

Target-4 is a water-cooled, 3-cm-diam, 7.5-cm-long tungsten cylinder. At an aspect angle of 30°, this source has an apparent width of 3.75 cm. The following equation gives us the simple geometric estimate of the source contribution to image resolution.

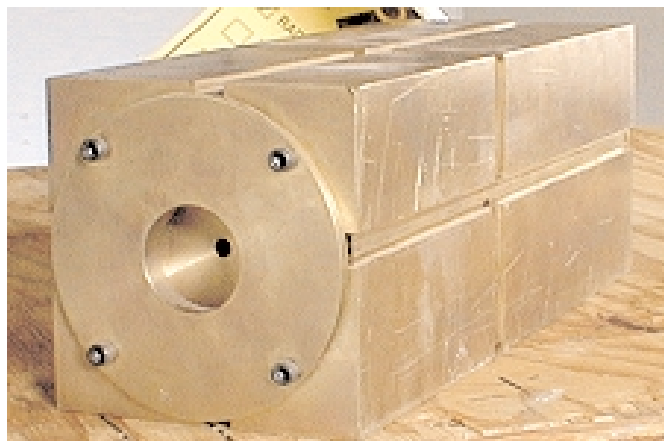
$$S1 = S0 (L1/L0),$$

where

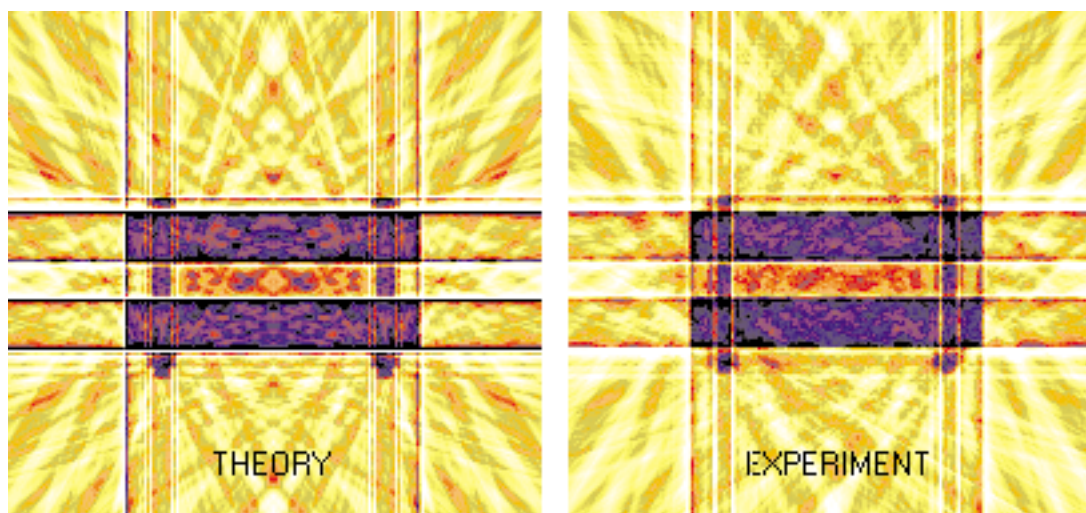
$S1$ = source contribution to image,
 $S0$ = apparent source size,
 $L0$ = source to object distance, and
 $L1$ = object to detector distance.

An object-to-detector separation $L1$ of 0.5 m therefore yields a source contribution to the image resolution of slightly less than 0.5 mm for a source-to-object distance of 40 m. From our edge profile measurements with the D_{38} cube, we found that an eight-layer stack of image plates yielded a total line-spread function with a Lorentzian shape and a FWHM (full-width at half-maximum) of approximately 0.75 mm. The pinhole image will allow a detailed deconvolution of the Target-4 source contribution, but a simple estimate based on the above geometric arguments suggests that the neutron resolution of the image-plate stack is about 0.5 mm.

Because CT imaging is our ultimate goal, we used the image-plate detectors to produce a trial CT image of a flat-plate test object. The object consisted of two 3/4-in. steel plates separated by 1/2-in. aluminum spacers and held together with two 1/4-in. bolts. A 32-mil-thick plastic drafting template with a series of circular holes was sandwiched between the two plates. We obtained a sequence of twelve images and reconstructed the cross section through the horizontal plane containing the two bolts (Fig. 3). The agreement between the experimental image and a calculated model using known total neutron cross sections was very good.



↑ **Fig. 2.** Brass collimator used to produce a neutron pinhole image of WNR Target-4. The collimator is 27 cm long with a central aperture that tapers to 1.6 mm in diameter at the center.



↑ **Fig. 3.** Flat-plate assembly used for CT-imaging experiments (top image). CT reconstruction from twelve views of a horizontal cross section through the two bolts (bottom image).

Additional calculations with this model show that at least 144 views will be required to see with confidence the holes in the plastic layer in a CT cross section. A single radiographic image of the plastic template is shown in Fig. 4.



↑ **Fig. 4.** Radiographic image of holes in a plastic drafting template shielded by iron.

We are currently working on producing a detailed CT image of a classified object using a portable D-T neutron generator and exploring new options for intense portable neutron sources. Also, an important development goal will be the selection of an imaging system—either a CCD imaging system or an amorphous-silicon panel—to replace the labor-intensive storage-phosphor plates, which require manual processing after every exposure. Both of these imaging systems will be able to electronically read out the image data without disturbing the physical placement of the detector. This capability will be an important feature for rapid, high-volume imaging.

Proton Radiography Experiments at LANSCE

M. Hockaday (P Division), Proton Radiography Team

PRAD at LANSCE is addressing weapons-physics issues for high explosives and material properties that result in materials being driven by high explosives. With this technique, high-energy protons impinge directly on an imploding or exploding object, interact with the material, and are scattered. Protons that exit the material strike a scintillator, which serves as a proton-to-light converter. The images are recorded with fast-gated cameras and are taken very quickly to freeze the motion of the moving components and features and to avoid motion blur. The proton pulse structure can be tailored to provide many frames to view the dynamic event and thereby produce a kind of "motion picture."

Los Alamos is leading a multilaboratory effort to demonstrate protons as a viable new radiographic probe to image exploding or imploding objects with high spatial and temporal resolution. The current PRAD effort being carried out in Area C has three main components: (1) to perform dynamic experiments or shots that meet the data needs of the weapons program; (2) to develop technology for better PRAD imaging, and (3) to provide a test bed for technology that will be required for the new AHF.

PRAD Experiments at LANSCE

In 1999, the PRAD team fired 13 high-explosive shots. In 2000, despite the Cerro Grande Fire, the team fired 28 shots bringing the total number of high-explosive shots to date to 78 since 1997. The LANSCE accelerator produced protons with 100% reliability for these experiments. In addition, beam time was used for advanced detector development, concept development, detector calibrations, and the radiographing of static mockups to determine shot configurations and design of experiments. In 2000, we also hosted an industrial collaborator for PRAD, the Ford Motor Company.

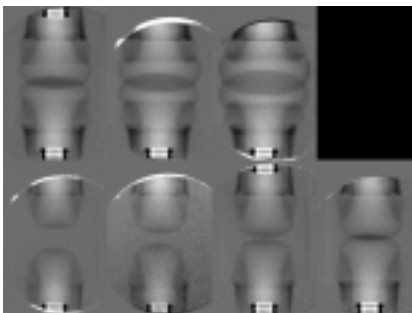
Thirteen shots in 1999 fell into three classes: (1) outside-user experiments, (2) high-explosive dynamic studies, and (3) implosion dynamic studies. For outside user experiments, we hosted SNL for three shots that investigated the functioning of voltage bars. High-explosive dynamic shots included further studies of hockey pucks and other geometries to investigate the formation of dead zones in high explosives. In one particular experiment, the Cambell-Cox corner turner, a small cylinder of high explosives was detonated into a

larger cylinder. As the detonation tried to turn the corner to the outside of the larger cylinder, dead zones were clearly visible in the PRAD images.

In 1999, we executed the first implosion experiment to be imaged with a proton beam. Billi G 2L was a collaborative effort with the Aldermaston Weapons Establishment (AWE) of the United Kingdom, and it required the joint efforts of LANSCE, P, X, ESA, ESH, and DX Division personnel. The chief scientific goals of the experiment were to study implosion-related phenomena relevant to the performance of nuclear weapons primaries and to further validate the capabilities of proton beams for radiographic imaging of nuclear-weapons hydrodynamic tests. Researchers recorded a time-sequenced series of radiographic images that essentially constitute a movie of the implosion over an extremely short span of time (less than 1/10,000 of a second). Fast electronic cameras viewed a picture formed in a radiation-to-light converter panel by protons. These protons survived passage through the Billi G device. The cameras used shutter speeds of only 60 billionths of a second to freeze the very fast motion of the device. The eleven-frame movie obtained of the implosion was the very first *greater than* two-frame radiographic sequence of a hydrotest implosion ever obtained.

The image quality and size that is possible with PRAD is dependent on the magnetic lens system used. Because protons are electrically charged, they undergo a large number of small-angle scatterings as they pass through an object. If not corrected, these scatterings blur the image as they pass from the object to be photographed to the recording medium. A series of four quadrupoles (devices that produce magnetic fields) was installed in Area C to focus protons onto the imaging plane. In addition, the power supplies of the existing magnets in experimental Area C were reconfigured so that a magnification of three could be achieved without having to move any magnets or purchase new power supplies. Under the auspices of LDRD funding, the power supplies were rewired, and a times-three magnifier was successfully demonstrated. In addition to the lens system, new detector schemes were developed to exploit the multiple-time-frame nature of PRAD. During 1999, an 8 x 8 pixel array was tested in Area C as a concept prototype for a *mega*-pixel detector that could be used in the new AHF. The array was tested using both ion-chamber and photodiode-array readouts, and the results were very encouraging.

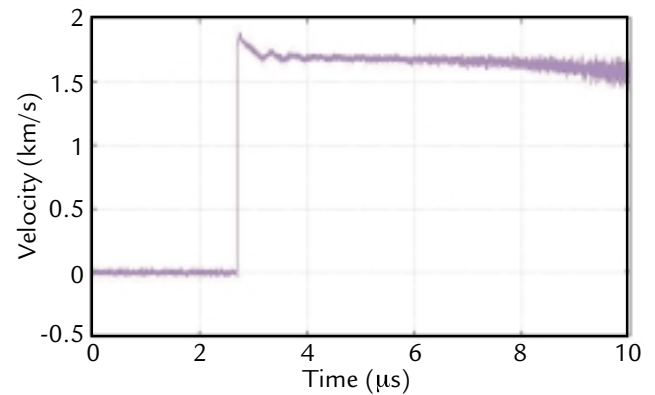
In 2000, the PRAD experimental repertoire included investigations of spall and ejecta phenomena, hydrodynamics, and the calibration of metal jets. For outside user experiments, we hosted SNL for an additional five shots that investigated the functioning of voltage bars with increased resolution. Additionally, six shots of the Hopyard experimental series (LLNL) were fired to look at ejecta phenomena. The ejecta phenomenon was also investigated with the fielding of the Dotson package. In addition to these shots, further dynamic studies of hockey pucks, corner turners, detonation wave shapers, and wave colliders were conducted, and two detonators were ignited simultaneously to obtain a radiograph of the interaction of two detonation waves (Fig. 1). Also a series of experiments were performed to determine the sheet thickness of a copper sheet jet as a function of time. This thickness is critical for obtaining an accurate temperature measurement using neutron resonance spectroscopy.



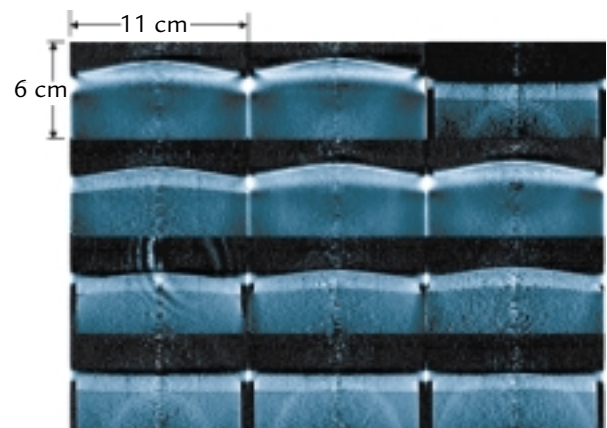
← **Fig. 1.** Ratio of dynamic over the static image that shows the collision and intersection of two detonation waves. The time sequence moves from lower left to the right and then up.

LDRD funding supported an effort to look at spall from aluminum plates driven by a hockey-puck high-explosive package. A critical aspect of this measurement was the development of a VISAR (Velocity Interferometer System for Any Reflector) capability to be used with PRAD. The VISAR provides an indication of spall and measures the surface velocity. A VISAR was configured and used successfully in one experiment (Fig. 2). Surface breakout was at $2.7 \mu\text{s}$ followed by oscillations typically seen on the surface of spalled material in an explosively driven configuration. Finally, the surface moves at a constant velocity of about $1.68 \text{ mm}/\mu\text{s}$. The oscillations correspond to a shock wave moving back and forth in a spall layer about 1.1 mm thick. Fig. 3 shows the radiographs taken during the experiment. The spall layer is first seen in the third image. The VISAR data provides a continuous surface velocity measurement between the radiographic frames. Final velocity of the surface (measured by the VISAR and radiographs) is $1.68 \text{ mm}/\mu\text{s}$.

In November 2000, the PRAD team obtained increased high-explosive load authorization from DOE, thus



↑ **Fig. 2.** VISAR velocity data.



↑ **Fig. 3.** Volume-density rendering of the eleven PRAD images of the VISAR and spall experiment. The upper right-hand image is a static taken before detonation. Time increases from the lower left to the top center image. The detonation shock wave in the high explosive can be seen in the three bottom images. Shock breakout is between the second and third images. The spall layer is visible in all images starting with the third. Time spacing between images is $1.073 \mu\text{s}$.

limiting experiments to a 10-lb TNT equivalent. Also in November 2000, the team performed the Billi G 4L as a second experiment to look at implosion dynamics. Camera components and the scintillator were changed to improve the statistics and resolution over that of Billi G 2L. The 16 separate images that formed a sixteen-frame movie of the implosion set a new world's record of frames obtained in the radiographic sequence of a hydrodynamic test.

The year 2000 was rounded out with the firing of a shot nicknamed Bambi. This experiment was one of several *local surrogate shots* that will lead up to the Stallion series of subcritical experiments using plutonium at the Nevada Test Site. The multi-time image data from the Bambi experiment will help us understand and model shock physics to ensure success with the Stallion series.

